Title
Link adaptation for wireless systems

Permalink
https://escholarship.org/uc/item/0h5955hf

Journal
Wireless Communications and Mobile Computing, 14(16)

ISSN
1530-8669

Authors
Tran, SV
Eltawil, AM

Publication Date
2014-11-01

DOI
10.1002/wcm.2292

Peer reviewed

RESEARCH ARTICLE

Link adaptation for wireless systems

Sang V. Tran and Ahmed M. Eltawil*

University of California Irvine, Irvine, CA, U.S.A.

ABSTRACT

To improve the robustness and reliability of wireless transmissions, two complementary link adaptation techniques are employed: adaptive modulation and coding (AMC) at the physical layer and hybrid automatic retransmission request (HARQ) at the medium access control layer. Because of their effectiveness in combating errors induced by the wireless channel, AMC and HARQ are now integral components of most emerging broadband wireless system standards, for example, LTE and WiMAX. Spectral efficiency (SE) as measured in bit per second per Hertz is one important parameter used to characterize a wireless system for comparison between different systems or between different configurations of the same system. This work provides a holistic approach of cross-layer optimizations with the intent of maximizing SE by combining AMC and HARQ. It formulates closed-form equations for calculating the average SE for wireless systems with the Rayleigh fading channel model. A new online algorithm is developed to optimize SE for both Rayleigh and non-Rayleigh fading channel. Simulations using proven LTE model are performed to compare SE obtained from closed-form equations and the developed algorithm for different system configurations. With the developed algorithm to determine how many retransmissions required in addition to the initial transmission in advance depending on the current wireless channel condition, the latency can be reduced up to 24 ms when sending the initial transmission and all of its retransmissions sooner than waiting for retransmission requests as is done previously. Copyright © 2012 John Wiley & Sons, Ltd.

*Correspondence

Ahmed M. Eltawil, University of California Irvine, Irvine, CA, U.S.A.
E-mail: aeltawil@uci.edu

1. INTRODUCTION

Wireless spectrum is a scarce resource, and how to use this resource efficiently has been the main driving requirement for all past, current, and future standards [1,2]. To obtain performance gains and to increase spectral efficiency (SE) of a system, the dependency between different protocol layers is often exploited to take advantage of the opportunistic communications and the multitude of operation modes available in the wireless link [3]. It opens new dimensions for research in cross-layer design and optimization.

The principle of adaptive modulation and coding (AMC) is to adaptively change the modulation and coding format with the variation of the wireless channel [4]. The receiver constantly measures the received signal-to-noise ratio (SNR) and block error rate (BLER), selects an appropriate modulation and coding scheme (MCS) from the available AMC set to meet the BLER requirement, and reports that selection (known as channel quality information (CQI)) to the transmitter through a feedback channel.

The transmitter uses the reported CQI in making its decision on using higher modulation scheme with higher bit rates when the channel condition is favorable [5]. Because of this benefit, AMC has become a *de-facto* standard at the physical (PHY) layer for emerging broadband wireless systems including 3GPP LTE [1] and WiMAX [2].

Furthermore, hybrid automatic retransmission request (HARQ) is widely adopted as another link adaptation (LA) technique at the medium access control (MAC) layer to improve the robustness of the wireless link. In HARQ systems, the receiver employs ACK/NACK protocol to inform the transmitter whether it receives the frame correctly or with error. This paper focuses on incremental redundancy (IR)-HARQ because of its effectiveness and popularity [6]. In IR-HARQ, the first transmission sends most systematic bits by puncturing out selected forward error correction (FEC) bits, and subsequent retransmissions send different combinations of systematic and FEC bits [1].

It was shown in [5] that by combining AMC and truncated ARQ, the SE can be improved under the prescribed delay and error performance constraints. However,

Liu *et al.* [5] did not take into account the progressive combining gain of HARQ. The authors in [7] took the same design approach as in [5] to evaluate the improvement in bandwidth (BW) efficiency achieved by the aggressive AMC with respect to the progressive combining gain in IR-HARQ with each retransmission. Various AMC and HARQ joint designs have been studied in literature focusing on single-link performance [8–11].

The main contributions of this paper can be summarized as follows:

(1) The paper generalizes the closed-form solution derived in [7] for single-link to multi-link (multiple antenna) systems in Rayleigh fading environments.

(2) This paper develops a new online framework to calculate SE for both Rayleigh and non-Rayleigh fading channels. This framework determines in advance how many retransmissions required and reduces the latency up to 24 ms when sending the retransmissions sooner than waiting for retransmission requests as is done previously.

(3) The complexity of the algorithm is quantified, and its performance is validated by simulation results.

(4) Simulation results are used to verify the increase in SE when jointly optimizing AMC and IR-HARQ for LTE system using both the closed-form and the proposed iterative framework.

The paper is organized as follows: The previous work is summarized in Section 2. The multiple-input multiple-output (MIMO) system model for AMC and IR-HARQ cross-layer optimizations (CLOs) design is described in Section 3. The CLO problem for algorithm development applicable to any wireless system is formulated in Section 4. The closed-form equation for joint AMC and IR-HARQ optimized design is developed in Section 5. An optimized algorithm to solve the problem formulated in Section 4 is described in Section 6. SEs of different system configurations are compared in Section 7. Finally, the paper's main points are concluded in Section 8.

2. PREVIOUS WORK

For Rayleigh fading channel, [7] and the references therein derived a closed-form equation to calculate SE for a single link. The idea is to partition the overall SNR range into $(M + 1)$ non-overlapping consecutive intervals, with SNR boundary points denoted as $\{\gamma_m\}_{m=0}^{M}$; that is, mode m is chosen when $\gamma = [\gamma_m, \gamma_{m+1})$. For closed-form solution, it is necessary to perform curve fitting the BLER into the exponential expression $a^* \exp(-g^*\gamma)$ where a and g are determined from the simulation results for each mode and each retransmission. The boundary points are then determined from the BLER and satisfied the packet loss constraint. The probability of selecting mode m is calculated

from the following equation:

$$\Pr(m) = \int_{\gamma_m}^{\gamma_{m+1}} p_\gamma(\gamma) d\gamma \quad (1)$$

where $p(\delta)$ is the probability density function (p.d.f.). The average BLER $\bar{P}_{m,n}$ corresponding to the nth retransmission of mode m is

$$\bar{P}_{m,n} = \int_{\gamma_m}^{\gamma_{m+1}} a_{m,n} e^{-g_{m,n}\gamma} p_\gamma(\gamma) d\gamma \quad (2)$$

where m defines mode index, $m = 1, 2, \ldots, M$, and n defines retransmission index, $n = 1, 2, \ldots, N$, where $n = 1$ is the initial transmission. The average BLER of the nth retransmission can be calculated as expressed in Equation (3) where R_m is mode m rate in bits/symbol.

$$\bar{P}_n = \frac{\sum_{m=1}^{M} R_m \bar{P}_{m,n}}{\sum_{m=1}^{M} R_m \Pr(m)} \quad (3)$$

The average number of retransmissions per block is then calculated as

$$\bar{N} = 1 + \sum_{i=1}^{N-1} \prod_{k=1}^{i} \bar{P}_k \quad (4)$$

$\bar{N}$ in Equation (4) can be a fractional number that will contribute to the difference between the theoretical result and the algorithmic result, which only allows for an integer number $\bar{N}$. Finally, the average SE as a function of number of retransmission $\bar{N}$ is determined by

$$S_e(N) = \frac{1}{\bar{N}} \sum_{m=1}^{M} R_m \Pr(m) \quad (5)$$

3. SYSTEM MODEL

Figure 1 depicts a MIMO system model with N_t transmit antennas and N_r receive antennas. The transmitter and receiver include a joint AMC and HARQ controller as one of its components [5]. The PHY layer constructs incoming MAC frames into PHY frames and transmits to the receiver through an air interface. The receiver estimates the channel based on the received SNR and BLER, and reports the CQI back to the transmitter. If the MAC layer receives a frame in error, the receiver's HARQ controller requests a retransmission from the transmitter following a defined ACK/NACK protocol. For PHY systems, the maximum number of retransmissions must be limited to a finite number denoted as $N - 1$. The system-specified design
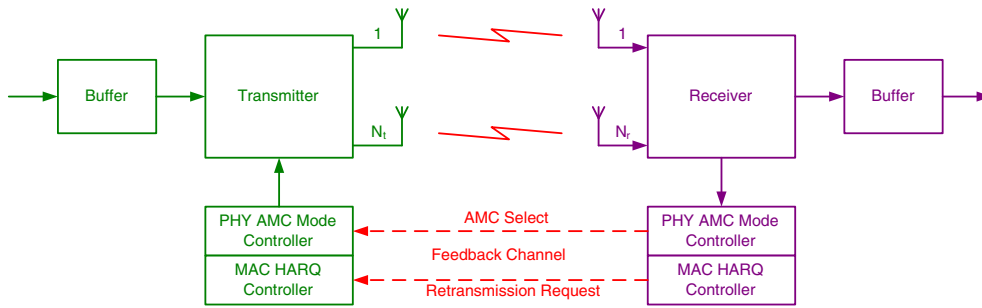
Figure 1. Multiple-input multiple-output system block diagram. PHY, physical; AMC, adaptive modulation and coding; MAC, medium access control; HARQ, hybrid automatic retransmission request.
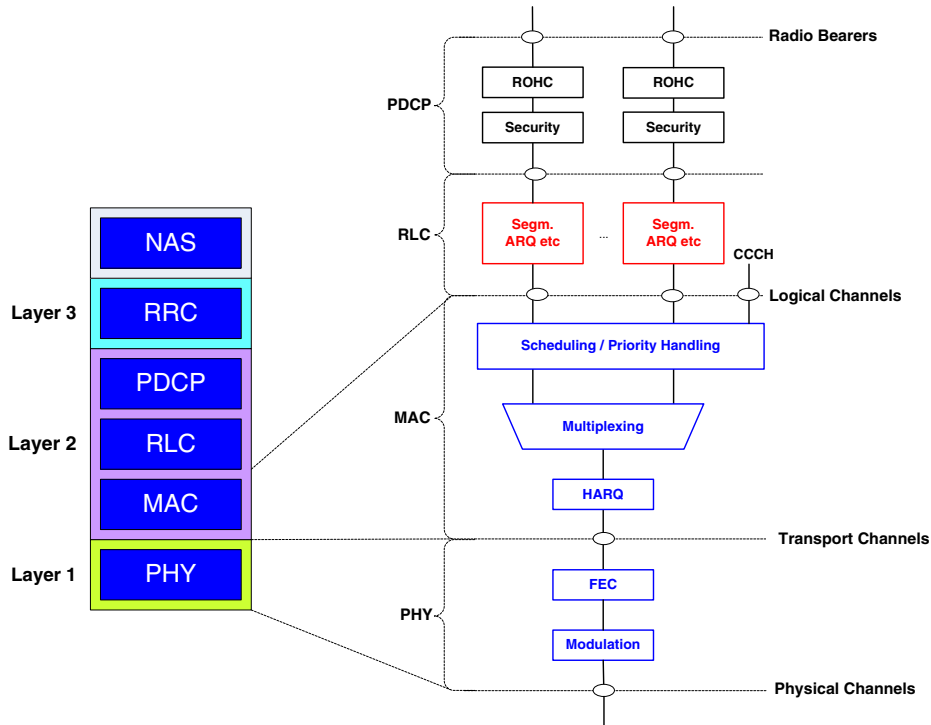

Figure 2. Simplified LTE protocol stack. PHY, physical; MAC, medium access control; HARQ, hybrid automatic retransmission request; FEC, forward error correction.

constraint is the probability of block loss specified as P_{loss} after $N - 1$ retransmissions.

If the $(N - 1)$th retransmission has occurred for the same transmitted block, the received signal vector at the kth transmission or $(k - 1)$th retransmission can be expressed as

$$\mathbf{r}_k = \mathbf{H}_k \mathbf{s}_k + \mathbf{n}_k, \quad k = 1, \ldots, N \qquad (6)$$

where $\mathbf{r}_k$ is the $N_r \times 1$ received signal vector, $\mathbf{H}_k$ is the $N_r \times N_t$ channel matrix, $\mathbf{s}_k$ is the $N_t \times 1$ transmitted signal vector, and $\mathbf{n}_k$ is the $N_r \times 1$ AWGN vector. $\mathbf{n}_k$ is assumed to be independent and identically distributed and zero mean circularly symmetric complex Gaussian. Because IR-HARQ is used, in general, $\mathbf{s}_k \neq \mathbf{s}_j$ for $k \neq j$ [6].

Figure 2 shows a simplistic view of the LTE protocol stack which is partitioned into access stratum (AS) and non-access stratum (NAS) [12] to illustrate the CLO concept. Layer 3 is the radio resource control (RRC), and layer 2 comprises of three sub-layers: the package data convergence protocol (PDCP), the radio link control (RLC), and the medium access control (MAC). The PDCP implements the robust header compression (ROHC) protocol to reduce transmission delay [13]. Scheduling and HARQ are the components of the MAC layer, and FEC and modulation are the components of the PHY layer. When the channel estimation is inaccurate, the transmitter may use a modulation scheme with a higher bit rate than what the channel can support. The receiver HARQ requests for retransmission of the block received in error in order to meet the

specified BLER. HARQ corrects occasional block errors, and it reduces AMC error control stringent requirements. In this regard, the HARQ complements the AMC to improve the BLER. The joint AMC-HARQ design outperforms either the design of AMC only or HARQ only.

Notations: N is the total number of transmissions including the first transmission and all the retransmissions, n is the retransmission index with $n = 1$ denotes the initial transmission, M is the number of modes available from AMC set, m is the AMC index, N_t is the number of transmit antennas, N_r is the number of receive antennas.

4. PROBLEM FORMULATION

The CLO can be formulated as an optimization problem where the objective is to select a joint strategy across multiple layers. This paper focuses on the AMC aspect of the PHY layer and the HARQ of the MAC layer. The different modes for $AMC_m, m = 1, 2, \ldots, M$ represents the various MCSs which translate into different rates that the PHY layer can support, for example, Table I. The different modes for $HARQ_n, n = 1, 2, \ldots, N$, represent different number of retransmission. In a real-time system, the block of data has to arrive at the receiver with a delay specified as D_{max}. The joint CLO problem can be formulated as follows:

Maximize   *Average spectral efficiency*

Subject to $BLER \leq P_{loss}$

$$D \leq D_{max}$$

$$\Omega = \sum_{n=1}^{N} M^n \; different \; joint \; design \; strategies$$

(7)

Table I. LTE channel quality information (CQI) table.

CQI index	Modulation	Efficiency
1	QPSK	0.1523
2	QPSK	0.2344
3	QPSK	0.3770
4	QPSK	0.6016
5	QPSK	0.8770
6	QPSK	1.1758
7	16QAM	1.4766
8	16QAM	1.9141
9	16QAM	2.4063
10	64QAM	2.7305
11	64QAM	3.3223
12	64QAM	3.9023
13	64QAM	4.5234
14	64QAM	5.1152
15	64QAM	5.5547

QPSK, quadrature phase-shift keying; QAM, quadrature amplitude modulation.

The LTE simulation engine used throughout this paper is based on that presented in [14]. Theoretical expressions derived within the paper are then compared with simulation results to validate the effectiveness and correctness of the proposed approach.

5. AMC AND HARQ JOINT OPTIMIZATION DESIGN

The procedure to calculate SE for each configuration, no retransmission, one retransmission, or two retransmissions, is summarized as follows:

(1) Obtain BLER versus SNR values from simulation for all modes and all retransmissions.
(2) BLER curve fitting from simulation for mode m transmission n, one curve each, to determine parameters $a_{m,n}$, $g_{m,n}$, and $\gamma_{m,n}$ [7].

$$P_{m,n}(\gamma) \approx \begin{cases} 1, & \text{if } 0 < \gamma < \gamma_{m,n} \\ a_{m,n} \exp(-g_{m,n}\gamma), & \text{if } \gamma \geq \gamma_{m,n} \end{cases}$$

(8)

(3) For each configuration, determine boundary SNRs $\{\gamma_m\}_{m=0}^{M}$ [7].

$$\gamma_m = \begin{cases} 0, & m = 0 \\ \dfrac{-1}{\sum\limits_{n=1}^{N} g_{m,n}} \ln\left(\dfrac{P_{loss}}{\prod\limits_{n=1}^{N} a_{m,n}}\right), & 0 < m < M \\ +\infty, & m = M \end{cases}$$

(9)

(4) For each transmission, calculate selected probability $\Pr(m)$ for mode m using Equation (1).
(5) Calculate the average BLER for the nth retransmission, mode m using Equation (2).
(6) Calculate the average BLER for the nth retransmission using Equation (3).
(7) Calculate the average number of transmissions per block using Equation (4).
(8) Calculate the average SE using Equation (5).

For LTE systems, Table I from [1] illustrates 15 different CQIs (AMC modes, $M = 15$), the associated modulation scheme, and the effective bit rate (efficiency) for each CQI.

The LTE simulation model described in [14] is run to obtain BLER versus SNR for the initial transmission, and the first and second retransmissions for all 15 CQIs. Figure 3 plots the BLER versus average SNR for LTE single-input single-output (SISO) system configuration for a sampled subset of CQIs. From these curves, parameters $a_{m,n}$, $g_{m,n}$, and $\gamma_{m,n}$ used in Equation (8) can be determined as outlined in step 2 earlier with index m indicating one of 15 CQIs and index n indicating the initial transmission, first retransmission, or second retransmission. The channel is set for block Rayleigh fading, and it is assumed that the BLER is independent between the first transmission and subsequent retransmissions. The same $P_{loss} = 0.005$ is used to evaluate system SE. The dot,
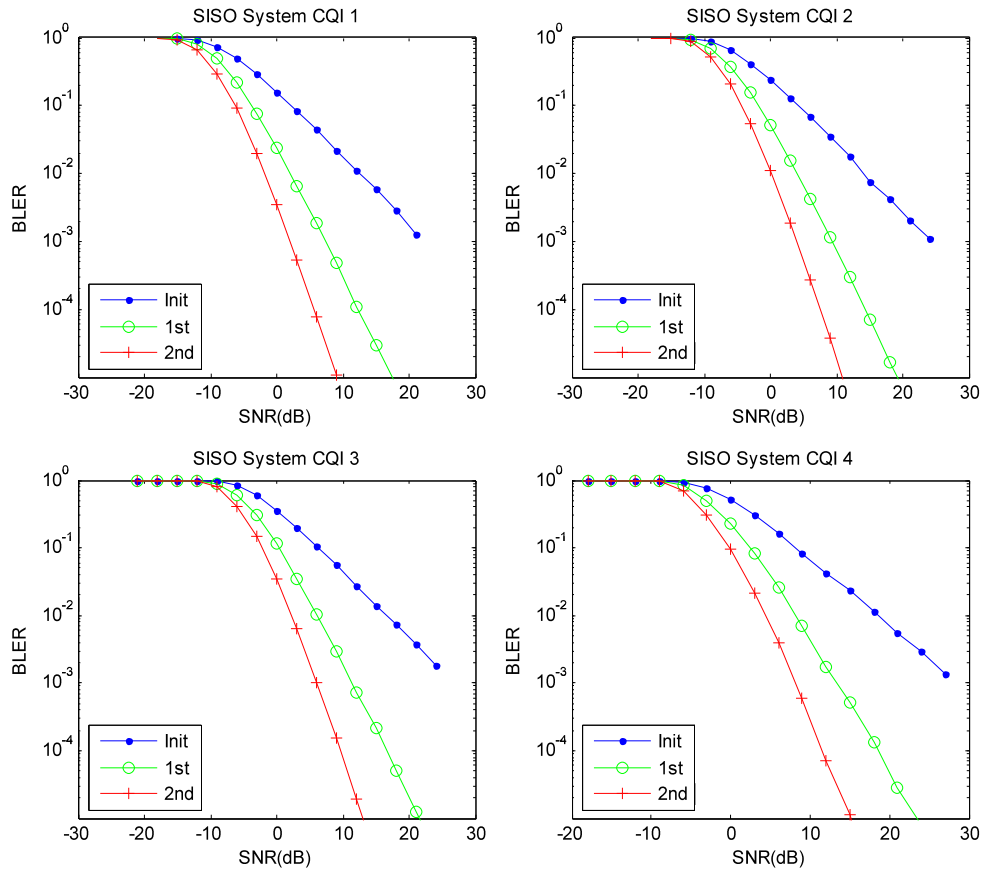
Figure 3. Single-input single-output (SISO) system block error rate (BLER) versus signal-to-noise ratio (SNR). CQI, channel quality information.

circle, and plus curves report the BLER results for initial transmission, first retransmission, and second retransmission, respectively. As can be seen from Figure 3, higher CQI provides higher bits per symbol but demands higher SNR. On average, to achieve the same BLER, CQI $(n + 1)$ requires about 2 dB more than CQI n. The performance gain from the initial transmission to the first retransmission is more significant than the performance gain from the first retransmission to the second retransmission in the high SNR region.

Figure 4 plots the CQI selection probability for the initial transmission of the described system. Below a certain SNR threshold (1 dB in Figure 4), transmission is prohibited because the channel is in deep fade. As SNR increases above the deep fade threshold, the lowest CQI associated with the lowest SE is selected for transmission. As the SNR continues to increase, a combination of different CQIs are selected for transmission to optimize the system effective SE. Eventually, the system will select the highest CQI (CQI 15) to achieve the highest SE when the SNR is high enough.

The works in [5] and [7] address only a single link (SISO) configuration. For MIMO configuration with N_t
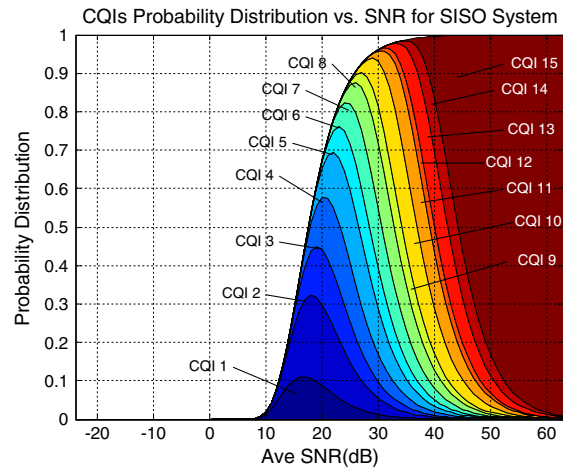

Figure 4. Single-input single-output (SISO) system initial transmission channel quality information (CQI) probability distribution. SNR, signal-to-noise ratio.

antennas at the transmitter and N_r antennas at the receiver, the order of diversity for the system is $N_t N_r$. The

distribution of γ is χ^2 with $2N_t N_r$ degree of freedom and can be expressed as [15]

$$p_\gamma(\gamma) = \frac{\gamma^{N_t N_r - 1} e^{-\gamma/\bar\gamma}}{\bar\gamma^{N_t N_r}(N_t N_r - 1)!}, \ \gamma \geq 0 \tag{10}$$

where $\bar\gamma$ is the average received SNR. From Equations (1) and (2) and after algebraic manipulation, $\Pr(m)$ and $\bar P_{m,n}$ can be derived as shown in Equations (11) and (12), respectively

$$\Pr(m) = e^{-\gamma_m/\bar\gamma} \sum_{k=1}^{N_t N_r} \frac{(\gamma_m/\bar\gamma)^{k-1}}{(k-1)!}$$
$$- e^{-\gamma_{m+1}/\bar\gamma} \sum_{k=1}^{N_t N_r} \frac{(\gamma_{m+1}/\bar\gamma)^{k-1}}{(k-1)!} \tag{11}$$

where $b_{m,n} = g_{m,n} + 1/\bar\gamma$. For $N_t = 1$ and $N_r = 1$, Equations (11) and (12) reduce to $\Pr(m)$ and $\bar P_{m,n}$ for single link derived in [7]. By substituting different values for N_t and N_r, $\Pr(m)$ and $\bar P_{m,n}$ can be calculated for different systems, for example, $N_t = 2$ and $N_r = 2$ for a 2×2 MIMO configuration. The SE can then be calculated from Equation (5).

The authors in [16] derive a cumulative distribution function (CDF) formula for a more restricted case with $N_r = 2$, that is, $N_t \times 2$ MIMO, for a beam-forming structure based on transmit MRC. The p.d.f. can be derived from the given CDF, and $\Pr(m)$ and $\bar P_{m,n}$ can be calculated as previously. It can be shown that this approach provides similar performance.

For multi-user case, the p.d.f. for U users can be obtained from Equation (10), as outlined in the Appendix, with subscript MU denoting multi-user:

$$p_{\gamma_{\mathrm{MU}}}(\gamma) = \frac{U(\gamma/\bar\gamma)^{N_t N_r - 1}}{\bar\gamma(N_t N_r - 1)!} e^{-\gamma/\bar\gamma} \left(1 - e^{-\gamma/\bar\gamma} \sum_{k=1}^{N_t N_r} \frac{(\gamma/\bar\gamma)^{k-1}}{(k-1)!}\right)^{U-1} \tag{13}$$

$\Pr(m)$, $\bar P_{m,n}$, and SE can then be derived different MIMO configurations, for example, configurations specified in LTE Rel. 8 ($N_t = 1, 2, 4$ and $N_r = 1, 2$). For instance, for a 2×2 MIMO system with two users,

$$\Pr(m) = \frac{1}{3\bar\gamma^4} \left[e^{-2\gamma_{m+1}/\bar\gamma} \sum_{k=1}^{4} \frac{1}{2\bar\gamma^{k-2}(k-1)!} \sum_{n=0}^{k+2} \frac{\bar\gamma^n(k+2)!}{2^n(k+2-n)!} \gamma_{m+1}^{k+2-n} - \bar\gamma e^{-\gamma_{m+1}/\bar\gamma} \sum_{k=0}^{3} \frac{6\bar\gamma^k}{(3-k)!} \gamma_{m+1}^{3-k} \right]$$
$$- \frac{1}{3\bar\gamma^4} \left[e^{-2\gamma_m/\bar\gamma} \sum_{k=1}^{4} \frac{1}{2\bar\gamma^{k-2}(k-1)!} \sum_{n=0}^{k+2} \frac{\bar\gamma^n(k+2)!}{2^n(k+2-n)!} \gamma_m^{k+2-n} - \bar\gamma e^{-\gamma_m/\bar\gamma} \sum_{k=0}^{3} \frac{6\bar\gamma^k}{(3-k)!} \gamma_m^{3-k} \right] \tag{14}$$

$$\bar P_{m,n} = \frac{a_{m,n}}{3\bar\gamma^4} \left[\frac{e^{-c_{m,n}\gamma_{m+1}}}{c_{m,n}} \sum_{k=1}^{4} \frac{1}{\bar\gamma^{k-1}(k-1)!} \sum_{n=0}^{k+2} \frac{(k+2)!}{c_{m,n}^n(k+2-n)!} \gamma_{m+1}^{k+2-n} - \frac{e^{-b_{m,n}\gamma_{m+1}}}{b_{m,n}} \sum_{n=0}^{3} \frac{6}{b_{m,n}^n(3-n)!} \gamma_{m+1}^{3-n} \right]$$
$$- \frac{a_{m,n}}{3\bar\gamma^4} \left[\frac{e^{-c_{m,n}\gamma_m}}{c_{m,n}} \sum_{k=1}^{4} \frac{1}{\bar\gamma^{k-1}(k-1)!} \sum_{n=0}^{k+2} \frac{(k+2)!}{c_{m,n}^n(k+2-n)!} \gamma_m^{k+2-n} - \frac{e^{-b_{m,n}\gamma_m}}{b_{m,n}} \sum_{n=0}^{3} \frac{6}{b_{m,n}^n(3-n)!} \gamma_m^{3-n} \right] \tag{15}$$

where $b_{m,n} = g_{m,n} + 1/\bar\gamma$, and $c_{m,n} = g_{m,n} + 2/\bar\gamma$.

$$\bar P_{m,n} = \frac{a_{m,n}}{(b_{m,n}\bar\gamma)^{N_t N_r}} \left[e^{-b_{m,n}\gamma_m} \sum_{k=1}^{N_t N_r} \frac{(b_{m,n}\gamma_m)^{k-1}}{(k-1)!} - e^{-b_{m,n}\gamma_{m+1}} \sum_{k=1}^{N_t N_r} \frac{(b_{m,n}\gamma_{m+1})^{k-1}}{(k-1)!} \right] \tag{12}$$

6. ALGORITHM

Section 5 provides closed-form equations to calculate SE for Rayleigh block fading channel. For other channel models, closed-form equations may not be available, and a heuristic approach must be sought. For any model, the BLER versus SNR can be obtained through simulations, calibrated with field trials, and made available in look-up table (LUT) format. Because the number of boundary SNRs is relatively small, for example, 16 for LTE system, the LUT size will be small. BLER values for intermediate SNR values can then be calculated by interpolation. The LUT can be either downloaded in real time or kept in non-volatile memory.

Each receiver measures the incoming data SNR and reports back to the transmitter. The transmitter uses this information to determine the strategy for the next transmission. The transmitter executes Algorithm 1 (described in Table II) to decide on the optimum transmission configuration strategy from the BLER requirements. The delay requirement dictates how many retransmissions can be used and when each retransmission needs to occur. It is possible to send the initial transmission and part or all of its retransmissions of the same block back to back or in the same time slot if the requirements are met. This allows the system to respond faster because the receiver can decode the block of data sooner, and the number of retransmission requests is minimized or can be alleviated altogether, and hence reduces the amount of traffic on the uplink channel. Another added benefit of sending both initial transmission and its corresponding retransmissions in advance is a simpler reordering of the received block process and less buffer space needed at the receiver. Each

transmission configuration t in Algorithm 1 is from the set of no retransmission ($t = 1$), one retransmission ($t = 2$), or up to $N - 1$ retransmissions ($t = N$). The selection of AMC mode m can be different for each transmission or retransmission within the same configuration t; for example, with one retransmission configuration, the AMC mode selection for initial transmission and first retransmission can be j and k, respectively, where $j \neq k$.

The accuracy of channel estimate will depend on the scheme used for CQI reporting or SNR reporting. For the proposed algorithm, because the same CQI reporting is applied to the original transmission and all corresponding subsequent retransmissions, CQI reporting is only required once, whereas it may be required to perform one CQI reporting for each original transmission and subsequent retransmissions in the existing scheme. Depending on the rate of change of the channel, there is a tradeoff between the uplink BW used to report CQI and the bit error rate because more frequent reports of CQI lead to better channel estimates albeit at the expense of BW and processing power.

Algorithm 1 returns the composite value (T_c, I) to indicate number of retransmission selected T_c, which takes on one of the t values defined earlier and the AMC value selected for each transmission or retransmission in the form of a t-tuple ($I_1, \ldots, I_t$), where $I_i, i = 1$ for initial transmission and $i = 2, \ldots, t$, indicates AMC mode for retransmission $i - 1$.

The scheduler at the eNodeB or base station allocates resources to users based on outcomes of the Algorithm 1 for each user. Figure 5 captures the dynamic of the mode and retransmission selection algorithm for LTE single user SISO system with $P_{\text{loss}} = 0.005$ and two retransmissions.

Table II. Selection algorithm detail.

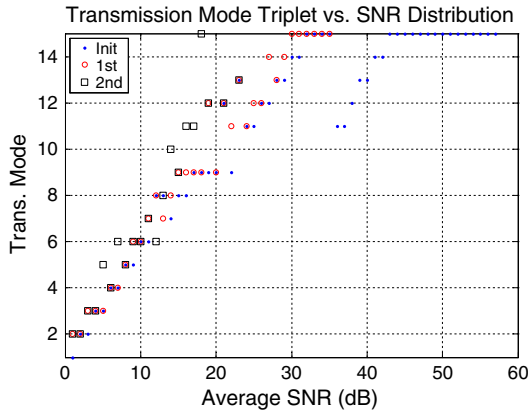|	
	Algorithm 1
1.	establish boundary points γ_n based on P_{loss} requirements
2.	receiver measures incoming data *SNR* and reports to transmitter
3.	initialize spectral efficiency $S_e = 0$
4.	for each transmission configuration $t = 1, \ldots, N$
5.	is this configuration satisfied *Delay* requirement? Yes, go to 6. No, go to 4
6.	for each retransmission $p = 1, \ldots, t$
7.	for each AMC mode $m = 1, \ldots, M$
8.	calculate effective target BLER based on measured $P_{\text{tar}} = \prod\limits_{p=1}^{t} BLER_{p,m}$
9.	if $P_{\text{tar}} \leq P_{\text{loss}}$
10.	calculate current spectral efficiency S_{curr}
11.	if $S_e < S_{\text{curr}}$
12.	$S_e = S_{\text{curr}}$
13.	$T_c = t$
14.	I = Index generating tuple ($I_1, \ldots, I_t$) for transmission t
15.	end if
16.	end if
17.	end for loop
18.	end for loop
19.	end for loop
20.	return (T_c, I)

Figure 5. Transmission mode selection.

Figure 6. Spectral efficiency comparison based on Algorithm 1. SISO, single-input single-output; SNR, signal-to-noise ratio.

It also illustrates the optimality of the CLO approach as explained later. At 1 dB, when the SNR is barely just over the threshold, the system selects the lowest rate with maximum number of retransmissions, that is, CQI 1 for initial transmission and CQI 2 for both the first and second retransmissions. As SNR increases to 2 dB, the system improves the SE by selecting CQI 2 for initial transmission. The system continues to use three transmissions with higher CQI as SNR increases to 20 dB where the system only needs to use two transmissions. At 21 dB, the system switches back to three transmissions with same CQI 12 for all transmissions because the effective rate of three transmissions at CQI 12 (3.9023/3) is higher than the effective rate of two transmissions at CQI 9 (2.4063/2) from Table I. At 36 dB, the system can satisfy the P_{loss} requirement with just one transmission, and the system continues to select one transmission with higher CQI as SNR increases to 43 dB where it achieves the highest SE using the highest CQI 15.

6.1. Design space exploration versus complexity

By exploring the total space of number of retransmissions in HARQ and the number of rates available in AMC, Algorithm 1 selects the highest rate that satisfies the P_{loss} requirement. The exploration space can be calculated as follows. For the system under consideration with 15 CQIs, there are three different scenarios to take into account: initial transmission only, initial transmission with one retransmission, and initial transmission with two retransmissions. For the initial transmission only case, because there is only one block to send, it can select 1 out of 15 different rates, there are 15 different combinations. For the second case with one retransmission, there are $15^2 = 225$ different combinations to consider. The last case with a total of three transmissions requires $15^3 = 3375$ combinations. The total consideration space for this case is 3615. The
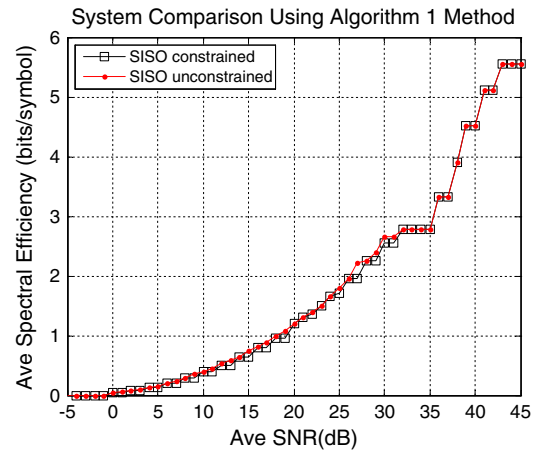
algorithm compares all 3615 cases and selects the highest rate that satisfies the BLER and delay requirements. In general, the exploration space can be derived as shown in Equation (16).

$$\sum_{i=1}^{N} M^i = \frac{M^{N+1} - M}{M - 1} \quad (16)$$

where N is the number of transmissions and M is the number of rates available. For an LTE system [1] supporting 15 CQI ($M = 15$) and three retransmissions configurations ($N = 4$), the space to consider is 54 240 combinations.

Figure 6 compares SE of single-user SISO system implementing Algorithm 1 under two different scenarios. The first scenario imposes a constraint of using the same AMC mode on the initial transmission and all subsequent retransmissions, whereas no such constraint is applied to the second scenario. The unconstrained method outperforms the constrained method by only 1 dB at low to mid SNR because of the larger space it considers. This suggests a hybrid method to take advantage of both methods, and Algorithm 1 can be further optimized. With the hybrid method, the system applies the unconstrained method to improve the SE at low SNR, and the system switches to the constrained method to reduce processing time and save power at high SNR. For the sub-optimum constraint method, the exploration space is reduced significantly to 45 (15*3), which increases linearly with M and N, compared with 3615, which increases exponentially with M and N as shown in Equation (16). This can be implemented easily as an LUT with a 45-word RAM. The LUT is updated according to feedback of channel condition and block loss rate requirement. For a typical implementation, for example, in a smart phone, a system may include a digital signal processor (DSP) or a microprocessor. It takes 45 compare operations or 90 ns, which is negligible compared with the 1 ms sub-frame time in LTE, to determine the optimum

MCS for a DSP operating at 500 MHz assuming that it takes one cycle to execute one compare operation. Depending on instructions available in the DSP instruction set, one comparison may take more than one cycle.

6.2. Scheduler considerations

The retransmission scheme described earlier can offer additional benefits and flexibility to the system scheduling. In general, the scheduling policy, based on quality of service (QoS), must take into account both fairness and deadline of packets that are transmitted to users for timing driven data as in voice, streaming video, and audio. In addition, for multi-media application, the timing relationship between video and audio must also be maintained for lip synchronization. For system applications, for example, the downlink of an LTE system, the eNodeB or base station has a certain throughput available for each frame that has to be distributed among all active users. The scheduler has to meet different conflicting requirements; it may have to give users with a certain level of required QoS higher priority even though the channel conditions for these users are not favorable, and at the same time attempting to maximize the system throughput. In LTE system, because a physical resource block, spanning 0.5 ms in the time domain and 180 kHz in the frequency domain, is the basic unit for resource allocation to users, the scheduler can exploit the potential gain of joint time and frequency scheduling. The CLO of AMC and HARQ with the joint time and frequency scheduling strategy provides the scheduler more flexibility in scheduling to optimize the time diversity gain from retransmission, spatial diversity gain from MIMO configuration, and multi-user diversity gain from a pool of users, and not all of them may need the system BW in the same time slot.

Figure 7 illustrates LTE downlink HARQ timeline and explains that the propagation delay and processing takes eight sub-frame time or 8 ms to complete transmission of one sub-frame and hence the reason why eight HARQ processes are implemented in LTE. When the user equipment (UE) receives the first sub-frame from the eNodeB (base station) after a propagation delay, it is required to generate an ACK sub-frame before the end of the fifth sub-frame in the eNodeB timeline. This allows approximately three sub-frame times (3 ms) for both the UE and the eNodeB to process the received data sub-frame and the ACK sub-frame, respectively.
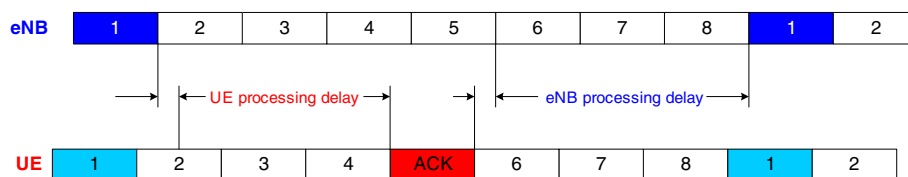
On the basis of the UE's feedback, the scheduler can determine the number of retransmissions needed for each UE and incorporate this information into scheduling in advance without waiting for retransmission request from the UE. For example, the initial transmission and subsequent retransmissions, up to three in LTE, can then be scheduled within the same sub-frame, which is 1 ms long in duration. This scheme reduces significantly the time delay of packets arrival at the receiver when the channel condition is not favorable. For LTE, because it requires an 8-ms window between one transmission and its next retransmission, the total additional delay for three retransmissions is 24 ms, which is significant enough to disrupt time critical applications. It also reduces the uplink BW usage required for request of retransmission of received error packets. In addition, the storage requirement at the transmitter allocated to buffer packets, which await acknowledgements from the receiver, may be alleviated altogether.

7. PERFORMANCE ANALYSIS

In this section, simulation results are presented for the closed-form formula derived in Section 5 based on the model described in Section 3. The block loss rate is set at $P_{loss} = 0.005$. Table III summarizes the simulation setup; see also [14]. The simulation is run for 25 000 frames to obtain BLER for each SNR value.

Figure 8 plots the number of retransmission versus SNR for both theoretical (Equation (4)) and practical approach

Table III. Simulation setup.

Parameter	Value
Carrier frequency	2.1 GHz
Bandwidth	1.4 MHz
No. of HARQ processes	8
Max. no. of HARQ retransmissions	3
Subcarrier spacing	15 kHz
Cyclic Prefix	Normal
Channel estimation method	Perfect
Channel interpolation method	Linear
Channel type	Flat Rayleigh, block fading
Propagation	NLOS
Uplink delay	1 TTI

HARQ, hybrid automatic retransmission request; NLOS, non-line-of-sight; TTI, transmission time interval.
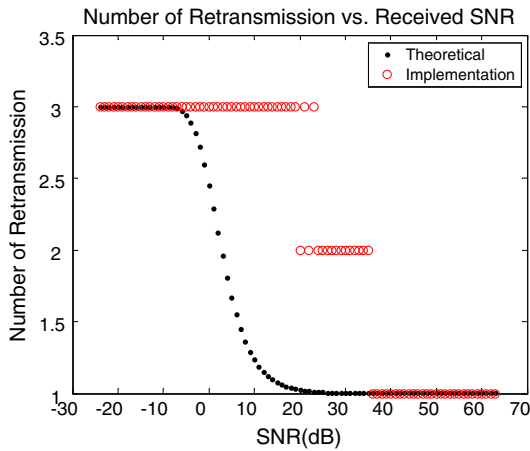

Figure 7. Hybrid automatic retransmission request timeline.

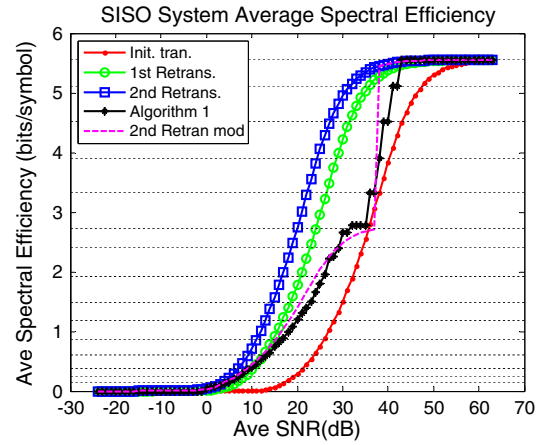**Figure 8.** Number of retransmission versus signal-to-noise ratio (SNR).

Figure 10. Spectral efficiency comparison of different single-input single-output (SISO) scenarios. SNR, signal-to-noise ratio.
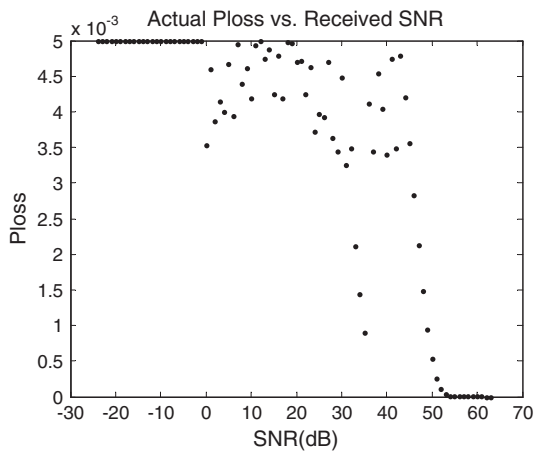

Figure 9. Actual P_{loss} versus signal-to-noise ratio (SNR) for Algorithm 1.

(Algorithm 1). In both cases the number of retransmission decreases from 3 to 1 as SNR increases. The number of retransmission derived in Equation (4) is allowed to take on non-integer values in contrast to the number of retransmission determined from Algorithm 1 can only take on integer values.

For the case of Algorithm 1, the number of retransmission at low SNR is three, oscillates between three and two depending on which configuration providing higher rate and settles at two in mid-range SNR, and switches to one transmission at high SNR. Because Algorithm 1 only allows integer number of retransmission, its actual P_{loss} is always better and with significant margins for some SNR values than the specified P_{loss} (0.005) as shown in Figure 9. For example, at 33 dB, it requires two retransmissions comparing to a small fraction larger than one retransmission in the theoretical case, but its P_{loss} is about 0.002, which is smaller than the required 0.005.

As is evident from Figure 10, there is a significant gain, as much as 12 dB, between the initial transmission and the first retransmission. A gain of 3.5 dB is achieved from the first retransmission to the second retransmission, but this gain is not as substantial as the gain from the initial transmission to the first retransmission. The horizontal dashed lines running across Figure 10 represent the SE of 15 CQIs listed in Table I. Figure 10 also shows the SE curve obtained from Algorithm 1 described in Section 6. For Algorithm 1 curve, above average SE of 2.73 (CQI 10), because there is no combination of multiple transmission can generate higher SE, the average SE jumps from one CQI SE value to the next CQI SE value for one transmission with no others average SE value in between, whereas there are other intermediate average SE values between two consecutive CQI SE values below CQI 10 SE value. Figure 5 indicates the number of transmission and the selected CQIs as explained previously; for example, at 21 dB, the system selects three transmissions at CQI 12 for an effective SE of 1.3 (3.9023/3) as shown in Figure 10. The difference between the theoretical curves and Algorithm 1 curve is due to the number of rates available is finite, and the number of retransmission is an integer number in Algorithm 1, whereas the number of retransmission can be a non-integer number as in Equation (4) for the theoretical case as illustrated in Figure 8. If the average number of retransmission in Equation (4) is limited to integer values by rounding it up to the next integer, the second Retrans. curve becomes the second Retran mod curve, which tracks the Algorithm 1 curve. The abrupt jump occurred in SE at 36 dB is due to the change from two transmissions to one transmission.

Figure 11 summarizes and compares the average SE of all the system configurations using Algorithm 1. The curves appear in steps because of the finite number of rates available. At 4 bits/symbol SE, the gain from SISO to 2×1 MISO, 1×2 SIMO, and 2×2 MIMO is 10, 13, and 18 dB, respectively.
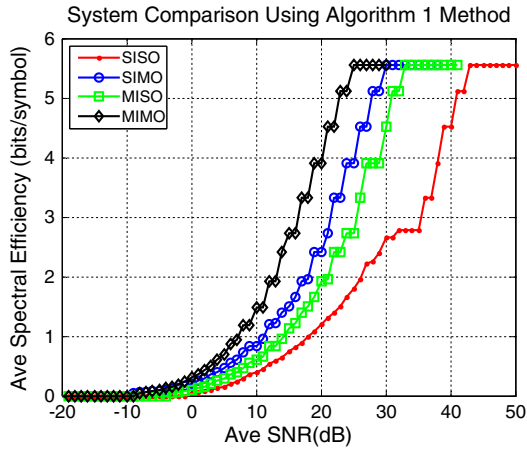
System Comparison Using Algorithm 1 Method

Figure 11. Spectral efficiency comparison using Algorithm 1. SISO, single-input single-output; SIMO, single-input multiple-output; MISO, multiple-input single-output; MIMO, multiple-input multiple-output.
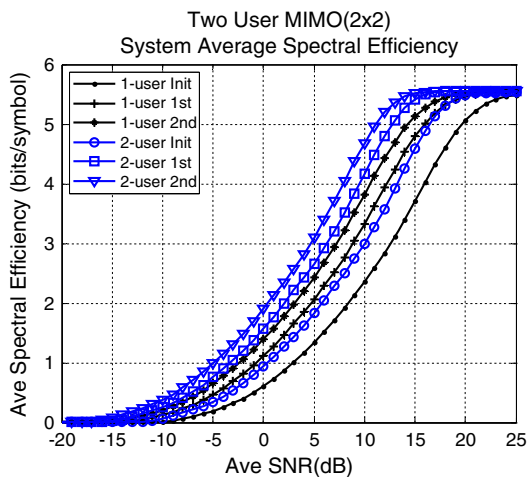
Two User MIMO(2x2) System Average Spectral Efficiency

Figure 12. Spectral efficiency for two users 2×2 multiple-input multiple-output (MIMO) system. SNR, signal-to-noise ratio.

Figure 12 compares SE between single-user system and two-user system. The two-user system has the advantage of multi-user diversity, and it provides and additional gain of about 3 dB comparing to single-user system for the same number of retransmission. The performance gain of time diversity from retransmission is greater than of multi-user diversity.

8. CONCLUSION

This paper investigates extensively the performance of different systems with CLO of AMC and finite number of retransmissions IR-HARQ. It provides closed-form equations for calculating the probability of mode selection, the average BLER, and the SE for wireless systems. An innovative algorithm is introduced as a new framework to calculate SE for system where closed-form equations are not available. Extensive simulation results using proven LTE model shown in this paper demonstrate the benefit of CLO in improving the average SE. With the developed algorithm to determine how many retransmissions required in addition to the initial transmission in advance depending on the current wireless channel condition, it is possible to send the initial transmission and part or all of its retransmissions sooner than waiting for retransmission requests as is done previously. This allows the system to respond faster, reduces the amount of traffic on the uplink channel, a simpler reordering of received block process and less buffer needed at the receiver. Channel estimation accuracy is a crucial factor in determining precisely the number of retransmissions. It will be interesting to study the channel estimation error rate for available wireless channel models and channel estimation techniques.

APPENDIX

The outage probability for a given threshold γ under MRC condition is given by [15]

$$P_{\text{out}} = P(\gamma_\Sigma < \gamma) = \int_0^\gamma p(\delta)\mathrm{d}\delta$$

$$= 1 - e^{-\gamma/\bar{\gamma}} \sum_{k=1}^{N_t N_r} \frac{(\gamma/\bar{\gamma})^{k-1}}{(k-1)!} \tag{A1}$$

where $p(\delta)$ is defined as in Equation (10). The outage probability of the MRC for U users for the target γ is

$$P_{\text{MU}}(\gamma) = \prod_{i=1}^{U} \left(1 - e^{-\gamma/\bar{\gamma}} \sum_{k=1}^{N_t N_r} \frac{(\gamma/\bar{\gamma})^{k-1}}{(k-1)!} \right) \tag{A2}$$

where the subscript MU indicates multiple user. The outage probability of the MRC for U users for the target γ with the same average received SNR for all users becomes

$$P_{\text{MU}}(\gamma) = \left(1 - e^{-\gamma/\bar{\gamma}} \sum_{k=1}^{N_t N_r} \frac{(\gamma/\bar{\gamma})^{k-1}}{(k-1)!} \right)^U \tag{A3}$$

The composite p.d.f. can be found by differentiating Equation (A3)

$$p_{\gamma_{\text{MU}}}(\gamma) = \frac{U(\gamma/\bar{\gamma})^{N_t N_r - 1}}{\bar{\gamma}(N_t N_r - 1)!} e^{-\gamma/\bar{\gamma}} \left(1 - e^{-\gamma/\bar{\gamma}} \sum_{k=1}^{N_t N_r} \frac{(\gamma/\bar{\gamma})^{k-1}}{(k-1)!} \right)^{U-1} \tag{A4}$$

which is Equation (13). It is tedious but straight forward to derive $\Pr(m)$ and $\bar{P}_{m,n}$ as formulated in Equations (1) and (2), respectively. Equations (14) and (15) can be derived with the help of the following result from [15].

$$\int_0^\gamma p(\delta)\mathrm{d}\delta = 1 - e^{-\gamma/\bar{\gamma}} \sum_{k=1}^{N_t N_r} \frac{(\gamma/\bar{\gamma})^{k-1}}{(k-1)!} \qquad (A5)$$

with $p(\delta)$ is defined as in Equation (10).

ACKNOWLEDGEMENTS

REFERENCES

1. 3GPP TS 36.213 v8.5.0 (2008-12), Physical layer procedures.

2. IEEE Standard 802.16e-2005. Part 16: Air interface for fixed and mobile broadband wireless access systems, December 2005.

3. Srivastava V, Motani M. Cross-layer design: a survey and the road ahead. *IEEE Communications Magazine* 2005; **43**: 112–119.

4. Alouini M, Goldsmith A. Adaptive modulation over Nakagami fading channels. *Kluwer, Wireless Personal Communications* 2000; **13**(1–2): 119–143.

5. Liu Q, Zhou S, Giannakis G. Cross-layer combining of adaptive modulation and coding with truncated ARQ over wireless links. *IEEE Transactions on Wireless Communications* 2004; **3**(5): 1746–1755.

6. Jang E, Lee J, Lou H, Cioffi JM. On the combining schemes for MIMO systems with hybrid ARQ. *IEEE Transaction on Wireless Communications* 2009; **8**(2): 836–842.

7. Kang C, Park S, Kim J. Design of adaptive modulation and coding scheme for truncated hybrid ARQ. *SpringerLink, Wireless Personal Communications* 2009; **53**(2): 269–280.

8. Chen F, Lijun S, Meiya C, Dacheng Y. A Markov based method for modulation and coding scheme (MCS) selection with hybrid ARQ retransmission. *IFIP International Conference on Wireless and Optical Communications Networks* 2006: 1–5.

9. Huaping F, Chen F, Tingjie L. A threshold optimizing method based on Markov in AMC combined with HARQ. *International Conference on Wireless Communications, Networking and Mobile Computing* 2006: 1–5.

10. Peng X, Song M, Song J. Cross-layer design for adaptive modulation and coding with hybrid ARQ. *IEEE International Symposium on Microwave, Antenna, Propagation, and EMC Technologies for Wireless Communications* 2007: 138–141.

11. Kim D, Jung B, Lee H, Sung D, Yoon H. Optimal modulation and coding scheme selection in cellular networks with hybrid-ARQ error control. *IEEE Transactions on Wireless Communications* 2008; **7**(12): 5195–5201.

12. 3GPP TS 36.300 v9.1.0 (2009-09), Overall description.

13. Dahlman E, Parkvall S, Skold J, Beming P. *3G Evolution: HSPA and LTE for Mobile Broadband*. Academic Press: Burlington, MA, USA, 2008.

14. Mehlführer C, Wrulich M, Ikuno JC, Bosanska D, Rupp M. Simulating the long term evolution physical layer, In *Proceedings of the 17th European Signal Processing Conference (EUSIPCO 2009)*, Glasgow, Scotland, August 2009; 1471–1478.

15. Goldsmith A. *Wireless Communications*. Cambridge University Press: New York, NY, USA, 2005.

16. Park S, Lee H, Lee S, Lee I. A new beamforming structure based on transmit-MRC for closed-loop MIMO systems. *IEEE Transactions on Communications* 2009; **57**(6): 1847–1856.

AUTHORS' BIOGRAPHIES

Sang V. Tran received the BS degree (summa cum laude) and MS degree in electrical engineering from the University of California, Los Angeles. He received his PhD degree in electrical and computer engineering from the University of California, Irvine. His research interest is in the area of SoC design and performance analysis of wireless communications systems.

Ahmed M. Eltawil is an associate professor at the University of California, Irvine. He received the Doctorate degree from the University of California, Los Angeles, in 2003 and the MSc and BSc degrees (with honors) from Cairo University, Giza, Egypt, in 1999 and 1997, respectively. Since 2005, he has been with the Department of Electrical Engineering and Computer Science, University of California, Irvine. He is the founder and director of the Wireless Systems and Circuits Laboratory (http://newport.eecs.uci.edu/~aeltawil/). His current

research interests are in low-power digital circuit and signal processing architectures for wireless communication systems where he has published more than 90 technical papers on the subject, including four book chapters. Dr. Eltawil has been on the technical program committees and steering committees for numerous workshops, symposia, and conferences in the area of VLSI and communication system design. He has received several distinguished awards, including the NSF CAREER award in 2010 supporting his research in low-power systems. He is a member of the Association of Public Safety Communications Officials (APCO) and has been actively involved in efforts towards integrating advanced communication technologies in critical first responder networks.